Segmentation of Retinal Vessels Using Nonlinear Projections

Yongping Zhang[1,2], Wynne Hsu[2], and Mong Li Lee[2]

[1] School of Electronic and Information Engineering
Ningbo University of Technology
Ningbo, China
Zhangyp1963@yahoo.com

[2] School of Computing
National University of Singapore
3 Science Drive 2, Singapore
{whsu, leeml}@comp.nus.edu.sg

ABSTRACT

An automated method for blood vessel segmentation is presented in this paper. The approach uses the nonlinear orthogonal projection to capture the features of vessel networks, and derives a novel local adaptive thresholding algorithm for vessel detection. By embedding in a kind of image decomposition model, the selection of system parameter which reflects the size of concerned convex set is examined. This approach differs from previously known methods in that it uses matched filtering, vessel tracking or supervised methods. The algorithm was tested on two publicly available databases: the DRIVE and the STARE. By comparison with hand-labeled ground truth, good average accuracies are achieved for the both databases.

Index Terms—Retinal imaging, vessel segmentation, nonlinear orthogonal projection, image decomposition, parameter selection

1. INTRODUCTION

The quantitative analysis of vessels and optic disc on digital retinal images is an essential step in the diagnosis of eye diseases, such as Diabetic Retinopathy (DR), glaucoma, and myopia. Manual measurements through visual inspection are time-consuming, tedious or even impossible when the vascular network is complex, or the signal-to-noise is weak. Therefore, developing a tool to automate the process of analysis is important to overcome the disadvantages of visual analysis [1]-[15].

Automated approaches to blood vessel delineation in digital retinal images can be roughly divided into two main categories: synchronous network segmentation and single vessel tracking. The former synchronously classifies each pixel based on some local features, including matched filtering (e.g., [2], [3]), edge-based method (e.g., [4], [5]), local adaptive thresholding (e.g., [6]), wavelet transform [7] and morphological filtering [8], [9]. The tracking methods search a continuous vessel segment starting from a point given by manually or automatically, based on certain local properties [1], [10]-[13]. Beyond these, the work in [14] combines principal component analysis with neural network to classify image pixels, while [15] employs the feature vectors from ridge extraction and the kNN-classifier for vessel detection.

In this paper, we present a novel method for vessel network segmentation in the basis of nonlinear projections [16]. Nonlinear projection algorithm has been introduced to solve total variation minimization problems involved in image decompositions [16], [17]. The goal of image decompositions is to split an original image into two components: one for the structural part and the other for the textural part. Such a decomposition problem can be modeled by convex optimization scheme [16]-[21]. The fundamental idea of the nonlinear projection algorithm is to transform the original convex optimization problem to searching the projection of the given image function into a bounded convex ball of a Banach space, G space [21], [22].

In the present study, the oscillating components of retinal images are adopted to capture the features of blood vessel networks. Furthermore, a vessel detection algorithm is derived from the nonlinear projections. This is a new adaptive thresholding method compared with the variational image binarization algorithm introduced in [23]. Both methods perform automatic thresholding with threshold surfaces generated by using variational models.

In order to improve the segmentation results, morphological open operations are also applied for the post processing of the resulting binary images. Finally, the images from two publicly available databases, the DRIVE database [15] and the STARE database [2], are used to evaluate the method proposed.

The remainder of this paper is organized as follows. In Section 2, we describe the fixed point algorithm for estimating the nonlinear orthogonal projection of an image function onto a bounded closed convex set that consists of oscillating functions. We also discuss the problem of determining an optimal radius of the closed convex set. In Section 3, we detail the vessel detection algorithm. In Section 4, we present the evaluation of results. Finally, we conclude the paper in Section 5.

2. NONLINEAR PROJECTIONS

In this section, we will review some basic facts about nonlinear projections onto closed convex sets and variational image decompositions. A fixed point algorithm for computing the nonlinear projection and a method for determining the radius of a closed convex set which severs as a projective space will also be presented.

2.1 Projection onto a Convex Set

Let *H* be a Hilbert space, $X \subset H$ be convex, closed, and non-empty. For $g \in H$, we define $P_X g$, called the projection of *g* onto *X*, to be the optimum for

$$\min_{v \in X} \frac{1}{2}\|g - v\|^2 \quad . \tag{1}$$

That is, the minimizer is the closest point in *X* to *g*. An interesting property of the projection function is that for any $g \in H$ there is a unique optimum for (1).

In this work, we consider the discrete case and two dimensional digital images. All the functions will be 2-dimensional matrices of size $M \times N$. In order to capture the texture information, we will consider the projection onto a closed convex set consisted of oscillating functions.

Let X_0 be the space of functions with zero mean:

$$X_0 = \{v : \sum_{i,j} v_{i,j} = 0\} \quad . \tag{2}$$

It has been proven that the set X_0 identifies with the following set of functions [20]:

$$G = \{v : \exists \xi = (\xi_1, \xi_2) \in L^\infty \times L^\infty, s.t. \quad v = div\xi\}, \tag{3}$$

where div represents the divergence of a vector-valued function $div\xi = \partial\xi_1 / \partial x + \partial\xi_2 / \partial y$. On G, a Banach norm, so-called G norm, is defined as [21], [22]:

$$\|v\|_G = \inf\{\|\xi\|_\infty : v = div\xi\} \quad , \tag{4}$$

where $\|\xi\|_\infty = \max_{i,j} |\xi_{i,j}|$ and $|\xi_{i,j}| = \sqrt{(\xi_1)_{i,j}^2 + (\xi_2)_{i,j}^2}$. The set G with the corresponding G norm defined in (4) is called G space.

To get the textural part of an image *f*, a natural idea is to project the original image into a bounded subset of space G. For a non-negative constant μ, if we denote by G_μ the closed ball with radius μ:

$$G_\mu = \{v : v \in G, \|v\|_G \le \mu\}, \tag{5}$$

then G_μ is a closed convex subset of G.

2.2 Fixed Point Algorithm

Computing the projection $P_{G_\mu} f$ amounts to finding the solution of the following problem:

$$\min\{\|\mu div\xi - f\|_{L^2}^2 : \max_{i,j} |\xi_{i,j}| \le 1\}. \tag{6}$$

This problem can be solved by a fixed point algorithm: $\xi^0 = 0$, and

$$\xi_{i,j}^{n+1} = \frac{\xi_{i,j}^n + \tau(\nabla(div\xi^n - f/\mu))_{i,j}}{1 + \tau|(\nabla(div\xi^n - f/\mu))_{i,j}|}. \tag{7}$$

In [16], it has been proven that if $\tau \le 1/8$ then $\mu div\xi^n$ converges to $P_{G_\mu} f$ as $n \to \infty$.

In the past years, a popular variation model, so-called ROF model, has been applied for decomposing an image $f \in L^2(\Re^2)$ into a sum of two functions $u + v$, where $u \in BV(\Re^2)$ is a function of bounded variation, while $v \in L^2(\Re^2)$ is an oscillating function representing texture or noise [16]-[21]. The decomposition problem can be modeled by the following total variation minimization:

$$\min_{(u,v) \in BV \times L^2 / f = u+v} \left(\int |\nabla u| + \frac{\int v^2}{2\mu}\right), \tag{8}$$

where $\int |\nabla u|$ is the total variation of *u*, $\mu > 0$ is the regularization parameter, serving as a scaling level to separate the two terms. If we let $v = P_{G_\mu} f$, and $u = f - P_{G_\mu} f$, then *u* and *v* are the solution of (8). This was proven from standard convex duality theory [16].

The above notations imply that for a given constant μ we can embed the projection procedure into the decomposition procedure. In the next subsection, we will utilize this embedding to address the selection problem of the radius μ.

2.3 Radius Selection

The parameter μ determines the size of the convex ball G_μ and hence the property of the corresponding nonlinear projective. In the image decomposition model (8), μ serves as a regularization parameter to balance the bounded variation and the oscillating components. In [21], the supremum of μ has been given by introducing the concept of G norm.

In practice, there were some approaches for selection of regularization parameter, including adaptive iteration method [16], [18], scale related automatic method [24] and correlation graph-based selection method [17]. In this study, we employ the correlation between the bounded variation and oscillating components as a measure to select an optimal parameter. The correlation between $u = f - P_{G_\mu} f$ and $v = P_{G_\mu} f$ is defined as:

$$corr(u,v) = \frac{\mathrm{cov}(u,v)}{\sigma_u^2 \sigma_v^2}, \tag{9}$$

where σ_g^2 represents the variance of function *g*, $\mathrm{cov}(g,h)$ represents the covariance between functions *g* and *h*. It is easy to see that

$$|corr(u,v)| \le 1. \tag{10}$$

The ideal decomposition result should be that the two

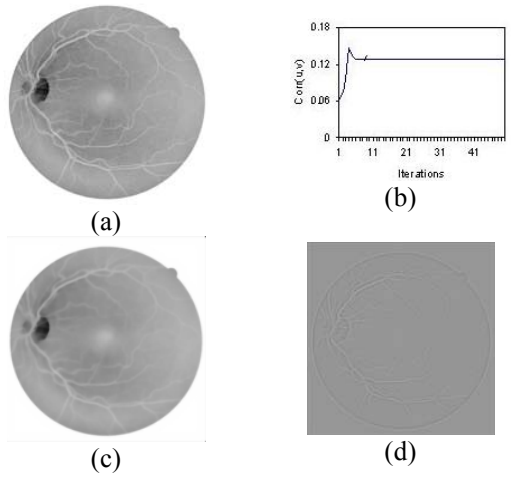

Fig. 1. An example for parameter selection. (a) Input image shown in Fig. 1(b). (b) Correlation graph. (c) and (d) are the corresponding components u and v + 150 using a better value of $\mu = 40$.

components are not correlated, that is, $corr(u,v) = 0$. As proved in [28], $corr(u,v) \geq 0$ holds for any positive μ. Hence we can select an optimal parameter μ based on minimizing the correlation. Fig. 1 shows an example. The correlation $corr(u,v)$ of 50 values of μ is plotted. The initial value of μ was set as $\mu^0 = 4$, and each time the value of μ was set as $\mu^n = 4 \cdot (n+1)$. After 50 iterations, a better value of $\mu = 40$ (corresponding to $n = 9$) was found.

In the next section, we will describe an algorithm for retinal vessel segmentation based on the above nonlinear projection.

3. VESSEL DETECTION ALGORITHM

From the notations above, the nonlinear projection can be used to capture the texture structures in images. In this approach, we employ the orthogonal projection to perform retinal blood vessel detection.

Motivated by the identical relationship between G and X_0, we get an automatic method to threshold the projective as:

$$Out_{i,j} = \begin{cases} 1, & (P_{G_\mu} f)_{i,j} > 0 \\ 0, & otherwise \end{cases}. \qquad (11)$$

This is equivalent to the global thresholding using the mean of projective as a threshold value, because $P_{G_\mu} f$ belongs to the set X_0. From the decomposition model (8) and the Proposition 2, the method is also equivalent to the following local adaptive thresholding with threshold surface u:

$$Out_{i,j} = \begin{cases} 1, & f_{i,j} > u_{i,j} \\ 0, & otherwise \end{cases}, \qquad (12)$$

since $P_{G_\mu} f = f - u$. In some means, this is a new variational image binarization algorithm in comparison with the method proposed in [23], where a multiscale variation model was introduced to generate smooth threshold surface.

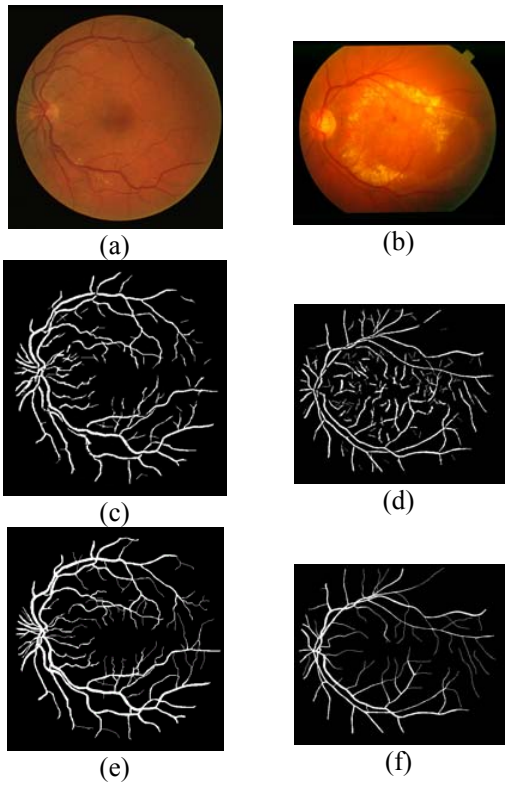

Fig. 2. Vessel segmentation on images from the DRIVE and STARE databases. First row: (a) original image from DRIVE database; (b) original image from STARE database. Second row: segmented images using our method. Bottom row: manual labeled results from DRIVE and STARE databases [15], [2].

After thresholding the projective, the morphological open operators are applied for removing blob-like structures and some shorter linear structures in the resulting binary image. In the experiments of this approach, the open operators with linear structural elements are applied to the binary image along twelve directions (0^o, 15^o, 30^o, …, and 165^o). The length of linear structure elements is set as 17 pixels. Our vessel detection algorithm can be summarized as the following steps:

Step 1: Choose a parameter μ, compute the orthogonal projective $P_{G_\mu} f$ using the fixed point algorithm (7).

Step 2: Threshold the projective as stating in (9) to get the output binary image *Out*.

Step 3: Apply morphological open operators to the binary image *Out* to remove blob-like structures and some shorter linear structures.

4. EXPERIMENTAL RESULTS

The 20 images from the test set of DRIVE database [15] and the 20 images from the website of STARE project [2] were used for evaluating our detection method. By examining the total of 40 images, the value of $\mu = 40$ can be employed as a common

optimal parameter for computing the nonlinear projection of images from the both databases.

As shown in Fig. 2, the detection results using our method and the manual labeled results from DIRIVE and STARE databases are compared. Using the manual labeled sets as reference, the values for the fraction of pixels erroneously detected as vessel pixels (false positive fraction, FPF) and for the fraction of pixels correctly detected as vessel pixels (true positive fraction, TPF) are examined; the average accuracy calculated with our method for the test sets are also investigated.

For the total of 20 images from STARE set, where half is normal and half is abnormal, the TPF, the FPF and the average accuracy are 0.9373, 0.0264 and 90.87%, respectively. On the data set, the average accuracy reported in [2] is 92.75%. The value reported by Jiang et al. in [6] is 90.09%.

On the DRIVE set, the experimental results show that 75.03 percent of the vessel pixels have been correctly detected, and the percentage of pixels erroneously classified is about 15.13. Meanwhile, an average accuracy of 96.40% is achieved. Based on the same database, the average accuracy reported in [15] is 94.41%.Using the method proposed in [6], the average accuracy is 89.11%.

5. CONCLUSION

The nonlinear projection algorithm has been recently applied to image processing and analysis. However, to our knowledge, there have been no published reports on the applications of nonlinear projections to retinal image analysis. In this paper, we have proposed a new approach to the automatic detection of retinal blood vessels based on nonlinear projections. The approach involved in selecting an optimal radius of the bounded convex set of oscillating functions. The radius can be also considered as the regularization parameter of ROF's image decomposition model. The experimental results indicate that to all the used images there is a common suited parameter for the procedure of nonlinear projection and a higher accuracy has achieved for the images from both the DRIVE and the STARE databases.

ACKNOWLEDGMENT

The authors would like to thank the authors of DRIVE and STARE databases for making their databases publicly available.

REFERENCES

[1] H. Li, W. Hsu, M. L. Lee, and H. Wang, "Automatic grading of retinal vessel calibre," *IEEE Transactions on Biomedical Engineering,* Vol. 52(7), pp.1352-1355, 2005.

[2] Hoover, V. Kouznetsova, and M. Goldbaum, "Locating blood vessels in retinal images by piecewise threshold probing of a matched filter response," *IEEE Transactions on Medical Imaging*, 19:203-210, March 2000.

[3] S. Chaudhuri, S. Chatterjee, et al., "Detection of blood vessels in retinal images using two-dimensional matched filters," *IEEE Transactions on Medical Imaging*, Vol. 8(3), pp. 263-269, 1989.

[4] M. E. Martínez-Pérez, A. D. Hughes, et al., "Retinal blood vessel segmentation by means of scale-space analysis and region growing," In *Medical Image Computing and Computer-assisted Intervention - MICCAI*, pp. 90-97, 1999.

[5] L. Gang, O. Chutatape, and S. M. Krishnan, "Detection and measurement of retinal vessels in fundus images using amplitude modified second-order Gaussian filter," *IEEE Transactions on Biomedical Engineering*, Vol. 49(2), pp. 168-172, 2002.

[6] X. Jiang and D. Mojon, "Adaptive local thresholding by verification-based multithreshold probing with application to vessel detection in retinal images," *IEEE Transactions on Pattern Analysis and Machine Intelligence*, Vol. 25(1), pp. 131-137, 2003.

[7] J. V. B. Soares, J. J. G. Leandro, et al., "Retinal vessel segmentation using the 2-D Gabor wavelet and supervised classification," *IEEE Transactions on Medical Imaging*, Vol. 25, pp. 1214-1222, 2006.

[8] F. Zana and J.-C. Klein, "Segmentation of vessel-like patterns using mathematical morphology and curvature evaluation," *IEEE Transactions on Meical. Imaging*, Vol. 11(7), pp. 1111-1119, 2001.

[9] Mendonca, and A. Campilho, "Segmentation of retinal blood vessels by combining the detection of centrelines and morphological reconstruction," *IEEE Trans. On Medical Imaging,* Vol. 25(9), pp. 1200-1213, 2006

[10] Can, H. Shen, J. N. Turner, et al., "Rapid automated tracing and feature extraction from retinal fundus images using direct exploratory algorithms," *IEEE Transactions on Information Technology in Biomedicine*, Vol. 3(2), pp. 125-138, 1999.

[11] Y. A. Tolias and S. M. Panas, "A fuzzy vessel tracking algorithm for retinal images based on fuzzy clustering," *IEEE Transactions on Medical Imaging*, Vol. 17(2), pp. 263-273, 1998.

[12] Chutatape, L. Zheng, and S. M. Krishnan, "Retinal blood vessel detection and tracking by matched Gaussian and Kalman filters," In *Proc. of the 20th Annual International Conference of the IEEE Engineering in Medicine and Biology Society, (EMBS'98)*, Vol. 20, pp. 3144-3149, 1998.

[13] X. Gao, A. Bharath, et al., "A method of vessel tracking for vessel diameter measurement on retinal images," In *ICIP01*, II, pp. 881-884, 2001.

[14] Sinthanayothin, J. Boyce, and C. T. Williamson, "Automated localisation of the optic disc, fovea, and retinal blood vessels from digital colour fundus images," *British Journal of Ophthalmology*, Vol. 83, pp. 902-910, 1999.

[15] J.J. Staal, M.D. Abramoff, et al., "Ridge based vessel segmentation in color images of the retina", *IEEE Transactions on Medical Imaging*, Vol. 23 (4), pp. 501-509, 2004.

[16] A. Chambolle, "An algorithm for total variation minimization and applications," J. *Mathematical Imaging and Vision*, Vol. 20, pp. 89-97, 2004

[17] J. F. Aujol, G. Gilboa, et al., "Structure-texture image decomposition - Modeling, algorithms, and parameter selection," *International Journal of Computer Vision*, Vol. 67 (1), pp.111-136, 2006.

[18] L. Rudin, S. Osher, and E. Fatemi, "Nonlinear total variation based noise removal algorithms," *Physica* D, Vol. 60, pp. 259–268, 1992.

[19] L. Vese and S. Osher, "Modeling textures with total variation minimization and oscillating patterns in image processing," *J. Scientific Comput*. Vol. 9, pp.553–572, 2003.

[20] J. F. Aujol, G. Aubert, et al., "Image Decomposition into a Bounded Variation Component and an Oscillating Component," *Journal of Mathematical Imaging and Vision*, Vol. 22(1), pp. 71-88, 2005.

[21] Meyer, *Oscillating patterns in image processing and in some nonlinear evolution equation*, The Fifteenth Dean Jacqueline B. Lewis Memorial Lectures. AMS, Boston, MA, USA, 2001.

[22] J.-F. Aujol and A. Chambolle, "Dual Norms and Image Decomposition Models," *International Journal of Computer Vision*, Vol. 63(1), pp.85-104, 2005.

[23] S. Tong, Y. Zhang, and N. Zheng, "Variational image binarization and its multiscale realizations," *J. of Mathematical Imaging and Vision*, Vol. 23, pp. 185-198, 2005.

[24] Strong and T. Chan, "Edge-preserving and scale-dependent properties of total variation regularization," *Inverse Problems*, Vol. 19(6), pp. 165-187, 2003.

[25] Strong, J.-F. Aujol and T. Chan, "Scale recognition, regularization parameter selection, and Meyer's G norm in total variation regularization," *SIAM Journal on Multiscale Modeling and Simulation*, Vol. 5(1), pp. 273-303, 2006.

[26] G. Gilboa, N. Sochen, Y. Y. Zeevi, "Estimation of optimal PDE-based denoising in the SNR sense," *IEEE Transactions on Image Processing*, Vol. 15(8), pp. 2269-2280, 2006.